

Energy-based Swing-up Control for a Two-link Underactuated Robot with Flexible First Joint

Zhiyu Peng (✉ 230208667@seu.edu.cn)

Southeast University <https://orcid.org/0000-0001-9591-9914>

Xin Xin

Okayama Prefectural University <https://orcid.org/0000-0002-0965-5930>

Yannian Liu

Southeast University

Research Article

Keywords: Underactuated system, energy-based controller, Acrobot, swing-up control, motion analysis, spring

Posted Date: April 20th, 2022

DOI: <https://doi.org/10.21203/rs.3.rs-1421307/v1>

License:  This work is licensed under a Creative Commons Attribution 4.0 International License.

[Read Full License](#)

Energy-based Swing-up Control for a Two-link Underactuated Robot with Flexible First Joint

Zhiyu Peng · Xin Xin · Yannian Liu

Received: date / Accepted: date

Abstract This paper concerns the swing-up control of an underactuated two-link robot with a linear torsional spring-attached first joint and an actuated second joint (called the FA robot below) moving in a vertical plane. First, we present a necessary and sufficient condition such the FA robot is linearly controllable at the upright equilibrium point (UEP, where two links are both upright). Second, we prove without any assumption that the FA robot is at an equilibrium point provided that its actuated joint angle is constant under a constant torque. Third, for the FA robot with its torsional stiffness of the spring being no greater than a value determined by the coefficients of its gravitational terms, we propose an energy-based controller without singular points to swing it up. We conduct a global motion analysis for the FA robot under the proposed controller. For the case that the total mechanical energy of the FA robot converges to its desired value, we present its phase portrait. For the case that the convergence is not achieved, we show that the FA robot approaches an equilibrium point belonging to a set of equilibrium points, and give a sufficient condition to check its stability. From the motion analysis, we present a sufficient condition such that the FA robot can be swung-up close to the UEP under the proposed swing-up controller. Finally, we verify our theoretical results through a numerical simulation.

This work was supported in part by the National Natural Science Foundation of China under grant number 61973077.

Zhiyu Peng
School of Automation, Southeast University, and Key Laboratory of Measurement and Control of Complex Systems of Engineering, Ministry of Education, Nanjing 210096, China
E-mail: 230208667@seu.edu.cn

Xin Xin
Faculty of Computer Science and Systems Engineering, Okayama Prefectural University,
Okayama 719-1197, Japan
E-mail: xxin@cse.oka-pu.ac.jp

Yannian Liu
School of Automation, Southeast University, and Key Laboratory of Measurement and Control of Complex Systems of Engineering, Ministry of Education, Nanjing 210096, China.
E-mail: 108109095@seu.edu.cn

Keywords Underactuated system · energy-based controller · Acrobot · swing-up control · motion analysis · spring

1 Introduction

An underactuated robot, which has less control inputs than its degrees of freedom (DOF), appears in a broad range of applications in real life because of its low energy consumption and simple structure. Among planar underactuated robots, the two-link robots with a single actuator are typical examples, which can be classified according to the actuator position into the Pendubot [8] and the Acrobot [5, 7]. For the Pendubot and the Acrobot moving in a vertical plane, many researchers concern a particular control problem called the swing-up control, i.e., driving the robot close to its upright equilibrium point (UEP, where the links are both upright) and stabilizing it at the UEP [3, 7, 13].

A flexible link presents advantages, for example, in space applications or assembly tasks [2, 4]. Since one can use a multi-link robot with torsional springs attached at the joints to model a flexible link [15], many researchers conduct studies on flexible links for practical or theoretical purposes [1, 3, 14, 16, 17]. For example, in the monograph [11], the authors studied several interesting examples of double pendulums with linear torsional springs introduced at the joints (hinge) (see, pp. 31–32, pp. 69–70, pp. 74–75, pp. 79–80).

In this paper, we study an underactuated two-link robot with a spring-attached first joint and an actuated second joint moving in a vertical plane, which can be regarded as the Acrobot with a linear torsional spring at the passive joint. We call it the FA robot, where “F” denotes “flexible” and “A” denotes “actuated”. Similarly, we use the AF robot to denote the Pendubot with a spring-attached passive joint. In the absence of gravity, the proportional derivative (PD) control can globally stabilize the AF robot at any desired equilibrium point [2]. However, in the vertical plane, the PD control can globally stabilize the AF robot at its UEP, only if the torsional stiffness is larger than a mechanical parameter related to a gravitational term of the robot [14]. Recently, in [1], the PD control in [14] is extended to globally stabilize the FA robot at its UEP, when the torsional stiffness is larger than a value determined by the coefficients of gravitational terms of the FA robot.

For the case that the torsional stiffness of the spring is no greater than the value mentioned above, this paper extends the energy-based control for the Acrobot in [13] to swing up the FA robot, since a PD controller can not stabilize it at the UEP. The basic idea of the energy-based controller is to control the total mechanical energy, the actuated joint angular velocity, and the actuated joint angle to their desired values respectively, thereby indirectly controlling the passive joint [3, 6, 13]. As shown in this paper, we encounter some new difficulties in the global motion analysis of the FA robot.

Firstly, we give a sufficient and necessary condition such that the linearized model of the FA robot at the UEP is controllable. We find that there exist some special mechanical parameters destroying the linear controllability. It is surprising because two extreme cases of the FA robot are always controllable at the UEP: the Acrobot (with the torsional stiffness being 0) is linearly controllable at its UEP

for any mechanical parameters [12]; if the torsional stiffness is ∞ , then link 1 is fixed at the upright position, and the robot is also controllable.

Secondly, we prove an important property of the FA robot that if the angle of the second joint is constant under a constant torque, then the angle of the first joint is also constant; that is, the FA robot is at an equilibrium point. This is a main result of this paper, which is useful in the motion analysis for the FA robot. There is a proof of this property in [1], however, the proof is based on several assumptions about mechanical parameters and the actuated joint of the FA robot. In this paper, we show that this property holds for any mechanical parameters, arbitrary actuated joint angle and torque.

Thirdly, we depict the motion of the FA robot under the energy-based controller by investigating the convergent value of the total mechanical energy, which is another main contribution of this paper. For the case that the total mechanical energy of the FA robot does converge to the desired value, we characterize the relationship between its mechanical parameters and its phase portrait. For the case that the convergence is not achieved, we show that the FA robot approaches an equilibrium point belonging to a set of equilibrium points, and we give a simple sufficient condition for checking its instability. Through the motion analysis, we present a sufficient condition such that the FA robot can be swung-up close to the UEP under the proposed swing-up controller.

The rest of this paper is organized as follows: In Section 2, the motion equation of the FA robot and the control objective are presented. Two important properties of the FA robot are presented in Section 3. Section 4 is about the controller design and the motion analysis. A simulation validation is provided in Section 5. Finally, a conclusion is made in Section 6.

2 Preliminaries

In this section, we give the motion equation of the FA robot moving in a vertical plane and the control objective.

2.1 Motion Equation

Consider the FA robot shown in Fig. 1. For link i ($i = 1, 2$), m_i is its mass, l_i is its length, l_{ci} is the distance between joint i and its center of mass (COM), and J_i is its moment of inertia with respect to its COM. There is a linear torsional spring attached at the first joint with torsional stiffness being k_1 and a torque τ acting on the second joint.

The motion equation of the FA robot is

$$M(q)\ddot{q} + H(q, \dot{q}) + G(q) + K(q) = B\tau, \quad (1)$$

where $q = [q_1, q_2]^T$ and

$$M(q) = \begin{bmatrix} M_{11}(q) & M_{12}(q) \\ M_{21}(q) & M_{22}(q) \end{bmatrix} = \begin{bmatrix} \alpha_1 + \alpha_2 + 2\alpha_3 \cos q_2 & \alpha_2 + \alpha_3 \cos q_2 \\ \alpha_2 + \alpha_3 \cos q_2 & \alpha_2 \end{bmatrix},$$

$$H(q, \dot{q}) = \alpha_3 \begin{bmatrix} -2\dot{q}_1\dot{q}_2 - \dot{q}_2^2 \\ \dot{q}_1^2 \end{bmatrix} \sin q_2,$$

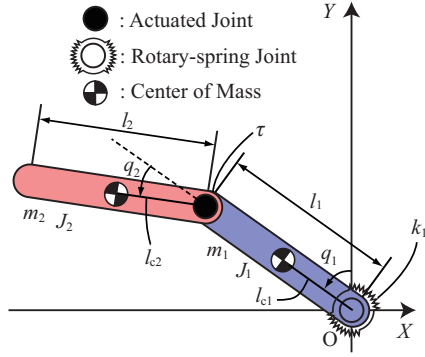


Fig. 1 The FA robot.

$$G(q) = \begin{bmatrix} -\beta_1 \sin q_1 - \beta_2 \sin(q_1 + q_2) \\ -\beta_2 \sin(q_1 + q_2) \end{bmatrix},$$

$$K(q) = [k_1 q_1, 0]^T, \quad B = [0, 1]^T,$$

$$\begin{cases} \alpha_1 = m_1 l_{c1}^2 + m_2 l_1^2 + J_1, \\ \alpha_2 = m_2 l_{c2}^2 + J_2, \quad \alpha_3 = m_2 l_1 l_{c2}, \\ \beta_1 = (m_1 l_{c1} + m_2 l_1) g, \quad \beta_2 = m_2 l_{c2} g, \end{cases} \quad (2)$$

with g being gravity acceleration.

Consider the mechanical energy of the FA robot. Let the gravitational potential energy $P_G(q)$ be zero at the X-axis shown in Fig. 1. We obtain

$$P_G(q) = \beta_1 \cos q_1 + \beta_2 \cos(q_1 + q_2). \quad (3)$$

Then, the potential energy $P(q)$ and the total mechanical energy $E(q, \dot{q})$ are respectively given by

$$P(q) = \frac{1}{2} k_1 q_1^2 + P_G(q), \quad (4)$$

$$E(q, \dot{q}) = \frac{1}{2} \dot{q}^T M(q) \dot{q} + P(q). \quad (5)$$

Let $q^e = [q_1^e, q_2^e]^T$ be an equilibrium configuration and τ^e be the corresponding equilibrium input. Substituting $q = q^e$, $\dot{q} = \ddot{q} = 0$ and $\tau = \tau^e$ into (1) yields

$$-\beta_1 \sin q_1^e - \beta_2 \sin(q_1^e + q_2^e) + k_1 q_1^e = 0, \quad (6)$$

$$-\beta_2 \sin(q_1^e + q_2^e) = \tau^e. \quad (7)$$

Recall an important property of the two-link planar robot about the five physical parameters in (2), which will be used in this paper.

Lemma 1 [13] For the system (1), the physical parameters defined in (2) satisfy

$$\alpha_2 \beta_1 > \alpha_3 \beta_2, \quad \alpha_3 \beta_1 \geq \alpha_1 \beta_2. \quad (8)$$

2.2 Control Objective

For mechanical parameters β_1, β_2 and the torsional stiffness k_1 of the FA robot, define γ as

$$\gamma = \frac{k_1}{\beta_1 + \beta_2} > 0. \quad (9)$$

For the case $\gamma > 1$ ($k_1 > \beta_1 + \beta_2$), in [1], a PD controller is designed for globally stabilizing the FA robot at the UEP. This paper studies how to design a controller so that the FA robot with $0 < \gamma \leq 1$ can be swung up and stabilized at the UEP.

3 Properties of the FA Robot

3.1 Linear Controllability

Take the state variable vector as $x = [q_1, q_2, \dot{q}_1, \dot{q}_2]^T$. When $x = 0$, the FA robot is at its UEP. The state equation of (1) is given by

$$\dot{x} = f(x) + g(x)\tau, \quad (10)$$

where

$$f(x) = \left[x_3, x_4, \frac{f_{3n}}{\alpha_1\alpha_2 - \alpha_3^2\cos^2x_2}, \frac{f_{4n}}{\alpha_1\alpha_2 - \alpha_3^2\cos^2x_2} \right]^T,$$

$$g(x) = \left[0, 0, \frac{-\alpha_2 - \alpha_3 \cos x_2}{\alpha_1\alpha_2 - \alpha_3^2\cos^2x_2}, \frac{\alpha_1 + \alpha_2 + 2\alpha_3 \cos x_2}{\alpha_1\alpha_2 - \alpha_3^2\cos^2x_2} \right]^T.$$

with

$$f_{3n} = \alpha_2(\beta_1 \sin x_1 - k_1 x_1) + \alpha_3 (\alpha_2(x_3 + x_4)^2 + \alpha_3 x_3^2 \cos x_2) \sin x_2 \\ - \alpha_3 \beta_2 \cos x_2 \sin(x_1 + x_2),$$

$$f_{4n} = -(\alpha_1 + \alpha_2 + 2\alpha_3 \cos x_2) (\alpha_3 x_3^2 \sin x_2 - \beta_2 \sin(x_1 + x_2)) \\ - (\alpha_2 + \alpha_3 \cos x_2) (\beta_1 \sin x_1 + \alpha_3 x_4(2x_3 + x_4) \sin x_2 + \beta_2 \sin(x_1 + x_2) - k_1 x_1).$$

Then, the following result can be obtained.

Lemma 2 Consider the torsional stiffness k_1 and physical parameters defined in (2). The linearized model of the FA robot at the UEP is controllable if and only if

$$k_1 \neq k_{uc} = \beta_1 - \frac{\alpha_1 + \alpha_3}{\alpha_2 + \alpha_3} \beta_2 > 0. \quad (11)$$

Proof. Note that $k_{uc} > 0$ holds due to (8). Linearize the system (10) around $x = 0$ to obtain

$$\dot{x} = Ax + N\tau, \quad (12)$$

where

$$A = \frac{1}{\Delta_0} \begin{bmatrix} 0 & 0 & \Delta_0 & 0 \\ 0 & 0 & 0 & \Delta_0 \\ \alpha_2\beta_1 - \alpha_3\beta_2 - \alpha_2k_1 & -\alpha_3\beta_2 & 0 & 0 \\ (\alpha_2 + \alpha_3)(k_1 - k_{uc}) & (\alpha_1 + \alpha_3)\beta_2 & 0 & 0 \end{bmatrix},$$

$$N = \frac{1}{\Delta_0} \begin{bmatrix} 0 \\ 0 \\ -\alpha_2 - \alpha_3 \\ \alpha_1 + \alpha_2 + 2\alpha_3 \end{bmatrix},$$

with

$$\Delta_0 = |M(0)| = \alpha_1\alpha_2 - \alpha_3^2 > 0.$$

For the linear system (12), the determinant of the controllability matrix $U_{ue} = [N, AN, A^2N, A^3N]$ is

$$|U_{ue}| = \frac{-(\alpha_1 + \alpha_3)^2(k_1 - k_{uc})^2}{\Delta_0^4}. \quad (13)$$

Thus, $|U_{ue}| \neq 0$ if and only if (11) holds. This completes the proof of Lemma 2. \square

We give the following remark about Lemma 2.

Remark 1 The Acrobot (the FA robot with $k_1 = 0$) is always linearly controllable around $x = 0$ [12]; when $k_1 \rightarrow \infty$, the angle of the first joint is fixed at $q_1 = 0$ and the system is clearly linearly controllable around $x = 0$. For the FA robot with $0 < k_1 < \infty$, it is interesting to find that some special mechanical parameters destroy the linear controllability.

3.2 Constant Active Joint Angle under Constant Torque

In this section, a property of the FA robot about its equilibrium configuration is presented, which is important for the motion analysis later.

Theorem 1 Consider the FA robot (1). If the angle of the second joint is constant under a constant torque, then the angle of the first joint is also constant, that is, the FA robot is at an equilibrium point.

Proof. Denote $q_2(t) \equiv q_2^*$ (“ \equiv ” means the equation holds for all time t) and $\tau(t) \equiv \tau^*$, where q_2^* and τ^* are constants. Substituting these equalities into (1) yields

$$M_{11}(q_2^*)\ddot{q}_1 - \beta_1 \sin q_1 - \beta_2 \sin(q_1 + q_2^*) + k_1 q_1 = 0, \quad (14)$$

$$M_{21}(q_2^*)\ddot{q}_1 + \alpha_3 \dot{q}_1^2 \sin q_2^* - \beta_2 \sin(q_1 + q_2^*) = \tau^*. \quad (15)$$

Since $M_{11}(q_2^*) > 0$ due to $M(q)$ being positive definite, we rewrite (14) as

$$\ddot{q}_1 = \frac{\beta_1 \sin q_1 + \beta_2 \sin(q_1 + q_2^*) - k_1 q_1}{M_{11}(q_2^*)}. \quad (16)$$

Eliminating \ddot{q}_1 in (15) by using (16), we have

$$\begin{aligned} & \frac{M_{21}(q_2^*) (\beta_1 \sin q_1 + \beta_2 \sin(q_1 + q_2^*) - k_1 q_1)}{M_{11}(q_2^*)} \\ & - \beta_2 \sin(q_1 + q_2^*) + \alpha_3 \dot{q}_1^2 \sin q_2^* - \tau^* = 0. \end{aligned} \quad (17)$$

Taking the derivative of (17) yields

$$\begin{aligned} & \dot{q} \left\{ \frac{M_{21}(q_2^*) (\beta_1 \cos q_1 + \beta_2 \cos(q_1 + q_2^*) - k_1)}{M_{11}(q_2^*)} \right. \\ & \left. - \beta_2 \cos(q_1 + q_2^*) + 2\alpha_3 \ddot{q}_1 \sin q_2^* \right\} = 0. \end{aligned} \quad (18)$$

Now, to show that $q_1(t)$ is constant, we use a contradiction argument. Suppose $\dot{q}_1(t) \neq 0$. Substituting \ddot{q}_1 in (16) into (18) and using $\dot{q}_1(t) \neq 0$, we obtain

$$\begin{aligned} & M_{21}(q_2^*) (-k_1 + \beta_1 \cos q_1 + \beta_2 \cos(q_1 + q_2^*)) - M_{11}(q_2^*) \beta_2 \cos(q_1 + q_2^*) \\ & + 2\alpha_3 \sin q_2^* (-k_1 q_1 + \beta_1 \sin q_1 + \beta_2 \sin(q_1 + q_2^*)) = 0. \end{aligned} \quad (19)$$

Taking the derivative of (19) and using $\dot{q}_1(t) \neq 0$, we obtain

$$\begin{aligned} & -M_{21}(q_2^*) (\beta_1 \sin q_1 + \beta_2 \sin(q_1 + q_2^*)) + M_{11}(q_2^*) \beta_2 \sin(q_1 + q_2^*) \\ & + 2\alpha_3 \sin q_2^* (-k_1 + \beta_1 \cos q_1 + \beta_2 \cos(q_1 + q_2^*)) = 0. \end{aligned} \quad (20)$$

Using trigonometric identities, we rewrite (20) as

$$A_0 \sin q_1 + B_0 \cos q_1 = 2\alpha_3 k_1 \sin q_2^*, \quad (21)$$

where

$$A_0 = 3\alpha_3 \beta_2 \cos^2 q_2^* - (\alpha_3 \beta_1 - \alpha_1 \beta_2) \cos q_2^* - (\alpha_2 \beta_1 + 2\alpha_3 \beta_2), \quad (22)$$

$$B_0 = (\alpha_1 \beta_2 + 2\alpha_3 \beta_1 + 3\alpha_3 \beta_2 \cos q_2^*) \sin q_2^*. \quad (23)$$

We claim

$$A_0 = 0, B_0 = 0. \quad (24)$$

Indeed, if (24) does not hold, we can rewrite (21) as

$$\sqrt{A_0^2 + B_0^2} \sin(q_1 + \omega(q_2^*)) = 2\alpha_3 k_1 \sin q_2^*, \quad (25)$$

where

$$\cos \omega = \frac{A_0}{\sqrt{A_0^2 + B_0^2}}, \quad \sin \omega = \frac{B_0}{\sqrt{A_0^2 + B_0^2}}. \quad (26)$$

Thus, (25) implies that $q_1(t)$ is constant, which contradicts the assumption that $\dot{q}_1(t) \neq 0$.

Now, we show that (24) can not hold. If (24) holds, from (21), (24) and $k_1 > 0$, we have $\sin q_2^* = 0$, that is, one of the following equations must be satisfied:

$$\cos q_2^* = 1, \quad (27)$$

$$\cos q_2^* = -1. \quad (28)$$

Firstly, suppose (27) holds. Substituting (27) into (22) yields

$$A_0|_{\cos q_2^*=1} = \alpha_1\beta_2 + \alpha_3\beta_2 - \alpha_2\beta_1 - \alpha_3\beta_1 = 0, \quad (29)$$

which contradicts Lemma 1. Thus, (27) can not hold.

Secondly, suppose (28) holds. Substituting (28) into (22) and using (24), we have

$$A_0|_{\cos q_2^*=-1} = (\alpha_3 - \alpha_1)\beta_2 + (\alpha_3 - \alpha_2)\beta_1 = 0. \quad (30)$$

Then, substituting (28) into (17), we obtain

$$\frac{(\alpha_1 - \alpha_3)\beta_2 + (\alpha_2 - \alpha_3)\beta_1}{\alpha_1 + \alpha_2 - 2\alpha_3} \sin q_1 - \frac{k_1(\alpha_2 - \alpha_3)q_1}{\alpha_1 + \alpha_2 - 2\alpha_3} = \tau^*. \quad (31)$$

This with (30) gives

$$-\frac{k_1(\alpha_2 - \alpha_3)q_1}{\alpha_1 + \alpha_2 - 2\alpha_3} = \tau^*. \quad (32)$$

Notice that $\alpha_2 - \alpha_3 \neq 0$ under (30). Otherwise, if $\alpha_2 - \alpha_3 = 0$, we have $\alpha_1 - \alpha_3 = 0$ from (30) and obtain $M_{11}(q_2^*)|_{q_2^*=\pi} = \alpha_1 + \alpha_2 - 2\alpha_3 = 0$, which contradicts the fact that $M_{11}(q_2) > 0$ for any q_2 . Hence, (32) implies that $q_1(t)$ is constant, which contradicts the assumption that $\dot{q}_1(t) \neq 0$. Thus, (28) can not hold.

Since the fact that neither (27) nor (28) holds raises a contradiction, we obtain that q_1 is constant. This completes the proof of Theorem 1. \square

We give the following two remarks on Theorem 1 in comparing the corresponding results in [1] and [13].

Remark 2 The content of Theorem 1 in this paper is the same as that of Lemma 1 in [1]; however, the proof in [1] needs an assumption described below. In [1], time derivative of (20) is taken and $A_0 \cos q_1 - B_0 \sin q_1 = 0$ is obtained instead of (21). To prove Theorem 1, an assumption that $A_0 \neq 0$, $B_0 \neq 0$ and $A_0 \neq B_0$ is introduced in [1]. In contrast to [1], Theorem 1 holds for any mechanical parameters, angle of the second joint, and constant torque.

Remark 3 A similar property of the Acrobot is proved in [13]. When $k_1 = 0$, for proving that (24) can not hold, $\cos q_2^* = -(2\alpha_3\beta_1 + \alpha_1\beta_2)/3\alpha_3\beta_2$ should also be considered in addition to (27) and (28). Moreover, if the physical parameters of the Acrobot satisfy (30), then $\tau^* = 0$ is obtained from (31) and $q_1 \equiv q_1^*$ does not hold. Thus, unlike the FA robot, Theorem 1 is not always satisfied for the Acrobot.

4 Swing-up Controller

In this section, for swinging up the FA robot, we propose an energy-based controller. In addition, we conduct a global motion analysis for the FA robot by studying energy convergence.

4.1 Controller Design

For E defined in (5), q_2 and \dot{q}_2 , we study how to design τ such that

$$\lim_{t \rightarrow \infty} E = E_r, \quad \lim_{t \rightarrow \infty} \dot{q}_2 = 0, \quad \lim_{t \rightarrow \infty} q_2 = 0, \quad (33)$$

where $E_r = \beta_1 + \beta_2$ is E evaluated at the UEP.

Take Lyapunov function V as

$$V = \frac{1}{2}(E - E_r)^2 + \frac{1}{2}k_D\dot{q}_2^2 + \frac{1}{2}k_Pq_2^2, \quad (34)$$

where $k_D > 0$ and $k_P > 0$ are constants. Using the property $\dot{E} = \dot{q}_2\tau$ and taking the time derivative of V along (1), we have

$$\dot{V} = \dot{q}_2((E - E_r)\tau + k_D\ddot{q}_2 + k_Pq_2). \quad (35)$$

If there exists τ satisfying

$$(E - E_r)\tau + k_D\ddot{q}_2 + k_Pq_2 = -k_V\dot{q}_2, \quad (36)$$

where $k_V > 0$ is a constant, then

$$\dot{V} = -k_V\dot{q}_2^2 \leq 0. \quad (37)$$

From (1), we obtain

$$\ddot{q}_2 = B^T\ddot{q} = B^T M^{-1} (B\tau - H - G - K). \quad (38)$$

Substituting (38) into (36) yields

$$\Lambda\tau = k_D B^T M^{-1} (H + G + K) - k_V\dot{q}_2 - k_Pq_2, \quad (39)$$

where

$$\Lambda = E - E_r + k_D B^T M^{-1} B. \quad (40)$$

If

$$\Lambda \neq 0, \quad \forall q, \forall \dot{q}, \quad (41)$$

then, from (39), we obtain

$$\tau = \frac{k_D B^T M^{-1} (H + G + K) - k_V\dot{q}_2 - k_Pq_2}{\Lambda}. \quad (42)$$

A lemma about the FA robot (1) under the controller (42) is presented here.

Lemma 3 Consider the FA robot (1) under the controller (42) with positive constants k_D, k_P and k_V . The controller (42) has no singular points for any (q, \dot{q}) if and only if

$$k_D > \max_{|q_1| \leq 2/\sqrt{\gamma}, q_2 \in [0, 2\pi]} \{(E_r - P(q_1, q_2)) M_p(q_2)\}, \quad (43)$$

where

$$M_p(q_2) = (B^T M^{-1} B)^{-1} = \frac{\alpha_1 \alpha_2 - \alpha_3^2 \cos^2 q_2}{\alpha_1 + \alpha_2 + 2\alpha_3 \cos q_2}. \quad (44)$$

In this case,

$$\lim_{t \rightarrow \infty} V = V^*, \lim_{t \rightarrow \infty} E = E^*, \lim_{t \rightarrow \infty} \dot{q}_2 = 0, \lim_{t \rightarrow \infty} q_2 = q_2^*, \quad (45)$$

where V^* , E^* and q_2^* are constants. Then, as $t \rightarrow \infty$, all closed-loop solutions (q, \dot{q}) approach an invariant set

$$W = \left\{ (q, \dot{q}) \mid q_2 \equiv q_2^*, \quad \dot{q}_1^2 = \frac{2(E^* - P(q_1, q_2^*))}{\alpha_1 + \alpha_2 + 2\alpha_3 \cos q_2^*} \right\}. \quad (46)$$

The proof of Lemma 3 is presented in Appendix A.

4.2 Motion Analysis

Now, we conduct the global motion analysis for the FA robot (1) under the controller (42).

Substituting $q_2 = q_2^e$, $\dot{q}_2 = \ddot{q}_2 = 0$, $E = P(q^e)$ and $\tau = \tau^e$ into (36) (from which we obtain the controller (42)) yields

$$(P(q^e) - E_r) \tau^e + k_P q_2^e = 0. \quad (47)$$

Therefore, the equilibrium configuration of the FA robot (1) under the controller (42) must satisfy (6), (7) and (47).

We present the following theorem.

Theorem 2 Consider the FA robot (1) under the controller (42) with $k_P > 0$, $k_V > 0$ and k_D satisfying (43). As $t \rightarrow \infty$, all solutions of the closed-loop system approach

$$W = W_r \cup \Omega, \quad \text{with} \quad W_r \cap \Omega = \emptyset, \quad (48)$$

where W_r is for $V^* = 0$, which is defined as

$$W_r = \left\{ (q, \dot{q}) \mid q_2 \equiv 0, \quad \dot{q}_1^2 = \frac{2(\beta_1 + \beta_2)(1 - \cos q_1) - k_1 q_1^2}{\alpha_1 + \alpha_2 + 2\alpha_3} \right\}, \quad (49)$$

and Ω is for $V^* \neq 0$, which is defined as

$$\Omega = \{(q^e, 0) \mid q^e \text{ satisfies (6), (7), (47), and } P(q^e) \neq E_r\}. \quad (50)$$

Proof. In the case $V^* = 0$, substituting $q_2^* = 0$, $E^* = E_r$ into (46) yields W_r defined in (49).

In the case $V^* \neq 0$, we obtain $E^* \neq E_r$. Otherwise, substituting $E \equiv E^* = E_r$, $\dot{q}_2 \equiv 0$ into (36) yields $q_2 \equiv 0$. Then, substituting $q_2 \equiv 0$ and $E = E_r$ into (34) yields $V^* = 0$, which introduces a contradiction. Thus, (36) implies that $\tau \equiv \tau^*$, which satisfies

$$(E^* - E_r) \tau^* + k_P q_2^* = 0, \quad E^* \neq E_r. \quad (51)$$

Then, according to Theorem 1, q_1 is also a constant. Therefore, the FA robot approaches the equilibrium set Ω in (50) as $t \rightarrow \infty$. \square

According to Theorem 2, we analyze W_r for $V^* = 0$ and Ω for $V^* \neq 0$ below.

4.2.1 The Phase Portrait of W_r

In this section, we give an analysis of the phase portrait of W_r defined in (49), which can help us to determine whether the FA robot (1) under the controller (42) can approach the UEP when $V^* = 0$. Since we have $q_2 \equiv 0$ in W_r , we only need to analyze the phase portrait of (q_1, \dot{q}_1) in W_r .

Rewrite the equation with respect to (q_1, \dot{q}_1) in W_r as

$$\frac{(\alpha_1 + \alpha_2 + 2\alpha_3)}{(\beta_1 + \beta_2)} \dot{q}_1^2 = F_1(q_1) - F_2(q_1), \quad (52)$$

where

$$F_1(q_1) = 2(1 - \cos q_1) = 4\sin^2\left(\frac{q_1}{2}\right) \quad (53)$$

is periodic with period 2π , and

$$F_2(q_1) = \gamma q_1^2 \quad (54)$$

with γ defined in (9).

Since the left side of (52) is non-negative, the solutions of (52) only exist in

$$D = \{q_1 \mid F_1(q_1) \geq F_2(q_1)\}. \quad (55)$$

Then, we give the following theorem.

Theorem 3 Let ψ_i ($i = 1, 2, \dots$) be a positive solution of

$$\tan\left(\frac{\psi}{2}\right) = \frac{\psi}{2}, \text{ with } 2i\pi < \psi < 2(i+1)\pi. \quad (56)$$

Define $\gamma_0 = 1$ and

$$\gamma_i = \frac{4}{4 + \psi_i^2}, \quad i = 1, 2, \dots \quad (57)$$

Consider

$$F_1(q_1) = F_2(q_1). \quad (58)$$

We have the following statements for the non-zero solutions of (58).

1). When $\gamma_i < \gamma < \gamma_{i-1}$ ($i = 1, 2, \dots$), Equation (58) has $4i - 2$ non-zero solutions:

$$\pm\phi_1(\gamma), \pm\phi_2(\gamma), \dots, \pm\phi_{2i-1}(\gamma), \quad (59)$$

with

$$\begin{cases} 0 < \phi_1(\gamma) < 2\pi, \\ 2(k-1)\pi < \phi_{2k-2}(\gamma) < \phi_{2k-1}(\gamma) < 2k\pi, \quad k = 2, 3, \dots, i. \end{cases}$$

2). When $\gamma = \gamma_i$ ($i = 1, 2, \dots$), Equation (58) has $4i$ non-zero solutions:

$$\pm\phi_1(\gamma_i), \pm\phi_2(\gamma_i), \dots, \pm\phi_{2i-1}(\gamma_i), \pm\psi_i, \quad (60)$$

with

$$k\pi < \phi_k(\gamma_i) < (k+1)\pi, \quad k = 1, 2, \dots, 2i-1.$$

Proof. Equation (58) holds if and only if

$$y_1 = y_2, \quad (61)$$

where

$$y_1 = \begin{cases} |\sin(q_1/2)|, & q_1 \geq 0, \\ -|\sin(q_1/2)|, & q_1 < 0, \end{cases} \quad y_2 = \sqrt{\gamma} (q_1/2).$$

Since y_1 and y_2 are both odd functions, we only need to analyze the positive solutions of (61). When $q_1 > 0$, y_1 is a periodic function and y_2 is a linear function, as depicted in Fig. 2.

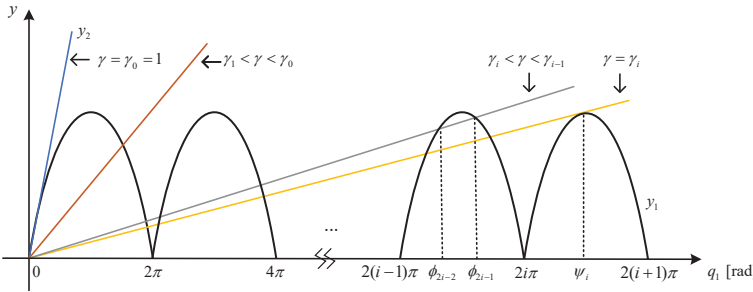


Fig. 2 y_1 and y_2 defined as (61).

Take $2i\pi < q_1 < 2(i+1)\pi$ ($i = 1, 2, \dots$) such that y_1 and y_2 are tangent. Therefore, from (61), we have

$$(-1)^i \sin\left(\frac{q_1}{2}\right) = \sqrt{\gamma}\left(\frac{q_1}{2}\right), \quad (62)$$

and the derivative of (62) is

$$(-1)^i \cos\left(\frac{q_1}{2}\right) = \sqrt{\gamma}. \quad (63)$$

Dividing both sides of (62) by the corresponding sides of (63), we obtain (56) with $q_1 = \psi_i$. Using $(62)^2 + (63)^2$ and letting $q_1 = \psi_i$, we find $\gamma = \gamma_i$ satisfying (57).

Regarding Statement 1), as shown in Fig. 2, when $\gamma_1 < \gamma < \gamma_0 = 1$, (61) has only one solution $q_1 = \phi_1(\gamma)$ in $(0, 2\pi)$. When $\gamma_i < \gamma < \gamma_{i-1}$ ($i = 2, 3, \dots$), (61) has a solution $q_1 = \phi_1(\gamma)$ in $(0, 2\pi)$; also, (61) has two solutions $q_1 = \phi_{2k-2}(\gamma), \phi_{2k-1}(\gamma)$ in $(2(k-1)\pi, 2k\pi)$ with $k = 2, 3, \dots, i$. Since y_1 and y_2 are odd functions, Statement 1) is true.

Regarding Statement 2), as shown in Fig. 2, when $\gamma = \gamma_i$ ($i = 1, 2, \dots$), (61) has one solution $q_1 = \phi_k(\gamma_i)$ in $(k\pi, (k+1)\pi)$ with $k = 1, 2, \dots, 2i-1$. Also, (61) has another solution $q_1 = \psi_i$ in $(2i\pi, 2(i+1)\pi)$. Since y_1 and y_2 are odd functions, Statement 2) is true. This completes the proof of Theorem 3. \square

According to Theorem 3, the relationship between the value of γ and the phase portrait of (q_1, \dot{q}_1) in W_r is illustrated as below.

1) If $\gamma_1 < \gamma < \gamma_0$, then the region defined in (55) satisfies

$$D = \{ |q_1| \leq \phi_1(\gamma) \}. \quad (64)$$

In this case, the phase portrait of (q_1, \dot{q}_1) in W_r consists of two loops connected at $(q_1, \dot{q}_1) = (0, 0)$ (see Fig. 3). Therefore, when $V^* = 0$, the closed-loop solutions can always approach the UEP.

2) If $\gamma_i < \gamma < \gamma_{i-1}$ ($i = 1, 2, \dots$), then

$$D = \bigcup_{k=1}^i \{ \phi_{2k-2}(\gamma) \leq |q_1| \leq \phi_{2k-1}(\gamma) \}, \quad (65)$$

where we define $\phi_0 = 0$ for achieving a unified expression. In this case, besides the two loops connected at $(q_1, \dot{q}_1) = (0, 0)$, there exist $2(i-1)$ isolated loops in the phase portrait of (q_1, \dot{q}_1) in W_r (see Fig. 4). The closed-loop solutions starting from some neighborhoods of these isolated loops can not approach the UEP.

3) If $\gamma = \gamma_i$ ($i = 1, 2, \dots$), then

$$D = \left\{ \bigcup_{k=1}^i \{ \phi_{2k-2}(\gamma_i) \leq |q_1| \leq \phi_{2k-1}(\gamma_i) \} \right\} \cup \{ |q_1| = \psi_i \}. \quad (66)$$

In this case, besides the two loops connected at $(q_1, \dot{q}_1) = (0, 0)$, there exist $2(i-1)$ isolated loops and two isolated equilibrium points in the phase portrait of (q_1, \dot{q}_1) in W_r . The closed-loop solutions starting from some neighborhoods of these isolated loops and equilibrium points can not approach the UEP.

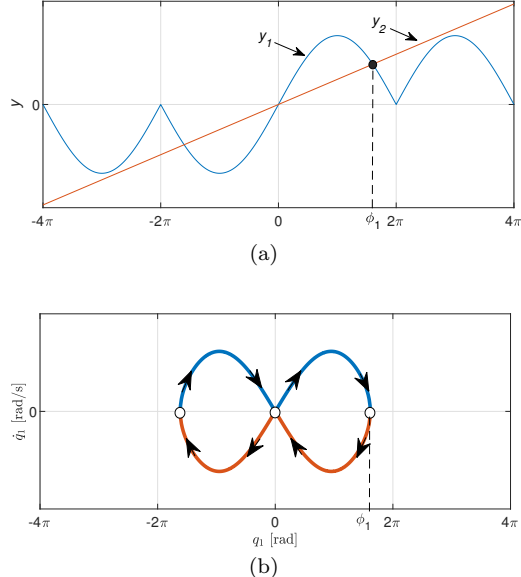


Fig. 3 When $\gamma_1 < \gamma < \gamma_0$, (a) ϕ_1 is the only positive solution of (58), (b) the phase portrait of (q_1, \dot{q}_1) in W_r .

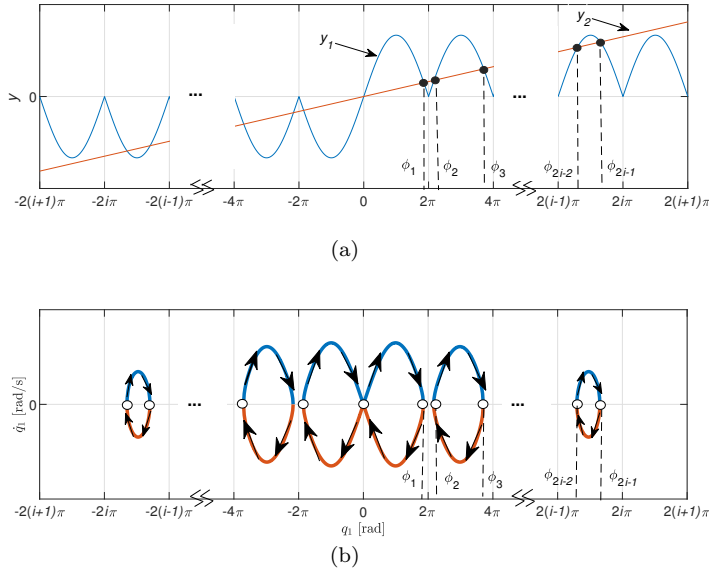


Fig. 4 When $\gamma_i < \gamma < \gamma_{i-1}$, (a) ϕ_{2k-2} and ϕ_{2k-1} ($k = 1, 2, \dots, i$) are the solutions of (58), (b) the phase portrait of (q_1, \dot{q}_1) in W_r .

For two special cases of the FA robot with $\gamma = \gamma_0 = 1$ or $\gamma = 0$, we give the following remark.

Remark 4 If $\gamma = 1$, we have $D = \{q_1 | q_1 = 0\}$ and W_r is reduced to the UEP. For the Acrobot (the FA robot with $\gamma = 0$), we have $D = \mathbb{R}$ and W_r is a homoclinic orbit, as depicted in Fig. 5. For these two special cases, the closed-loop solutions in W_r can always approach the UEP.

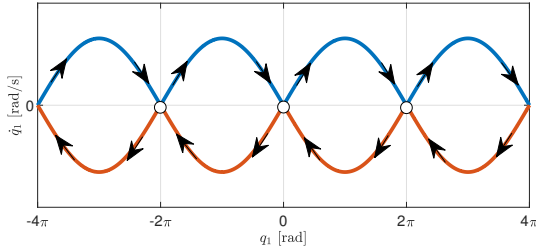


Fig. 5 The phase portrait of (q_1, \dot{q}_1) in W_r with $\gamma = 0$ over the domain $-4\pi < q_1 < 4\pi$.

4.2.2 The Stability of the Equilibrium Points in Ω

If an equilibrium point in Ω defined as (50) is unstable, then the FA robot can not be maintained at that point in practice due to some disturbances. Thus, we give a sufficient condition for checking the instability of the equilibrium points in Ω .

Lemma 4 Consider an equilibrium point $[q_1^e, q_2^e, 0, 0]^T \in \Omega$. The equilibrium point is unstable if

$$(k_1 - P_G(q_1^e, q_2^e)) (P(q_1^e, q_2^e) - E_r) < 0, \quad (67)$$

where $P_G(q_1^e, q_2^e)$ and $P(q_1^e, q_2^e)$ are defined as (3) and (4), respectively.

Proof. The equilibrium point $[q_1^e, q_2^e, 0, 0]^T$ is unstable if we have

$$V(q_1^e + \delta, q_2^e, 0, 0) < V(q_1^e, q_2^e, 0, 0), \quad (68)$$

where δ is a very small number. Indeed, if (68) holds, the FA robot starting from $[q_1^e + \delta, q_2^e, 0, 0]^T$ can not approach $[q_1^e, q_2^e, 0, 0]^T$ due to (37).

Firstly, consider the case that $P(q_1^e, q_2^e) < E_r$. Then, (67) is equivalent to

$$k_1 > P_G(q_1^e, q_2^e). \quad (69)$$

We can take sufficiently small δ such that $P(q_1^e + \delta, q_2^e) < E_r$ holds. Then, (68) is equivalent to

$$\Delta_P = P(q_1^e + \delta, q_2^e) - P(q_1^e, q_2^e) > 0. \quad (70)$$

Computing (3) $\times \cos \delta +$ (6) $\times \sin \delta$, we obtain

$$P_G(q_1^e + \delta, q_2^e) = -k_1 q_1^e \sin \delta + P_G(q_1^e, q_2^e) \cos \delta. \quad (71)$$

Also, we can calculate that

$$\frac{1}{2} k_1 (q_1^e + \delta)^2 = k_1 q_1^e \delta + \frac{1}{2} k_1 \delta^2 + \frac{1}{2} k_1 (q_1^e)^2. \quad (72)$$

According to the definition of P_G in (4), we have

$$\Delta_P = P_G(q_1^e, q_2^e) \times (\cos \delta - 1) + k_1 q_1^e (\delta - \sin \delta) + \frac{1}{2} k_1 \delta^2. \quad (73)$$

Taylor expanding (73) at $\delta = 0$ yields

$$\Delta_P = \frac{1}{2} (k_1 - P_G(q_1^e, q_2^e)) \delta^2 + o(\delta^2), \quad (74)$$

where $o(\delta^2)$ is the Peano form of remainder. Thus, $\Delta_P > 0$ when (69) holds.

Secondly, regarding the case $P(q_1^e, q_2^e) > E_r$, we can also prove similarly that (68) holds when $k_1 < P_G(q_1^e, q_2^e)$. Therefore, (68) holds if (67) is satisfied. This completes the proof of Lemma 4. \square

To illustrate under what conditions the FA robot (1) can be driven close to the UEP by the controller (42), we give the following theorem to summarize the results of the motion analysis.

Theorem 4 Consider the FA robot (1) under the controller (42) with $k_P > 0$, $k_V > 0$ and k_D satisfying (43). Regarding Ω defined in (50) and W_r defined in (49), we have the following two statements:

- 1) If all the equilibrium points in Ω satisfy (67), then all closed-loop solutions approach W_r as $t \rightarrow \infty$.
- 2) If $\gamma_1 < \gamma \leq 1$, all closed-loop solutions in W_r can approach the UEP (see Fig. 3(b)).

4.3 Stabilizing Control

For the FA robot (1) under the controller (42) with positive k_V, k_P, k_D , define J_{uep} as the Jacobian matrix evaluated around the UEP. Computing the characteristic equation of J_{uep} yields

$$(k_P + k_V s + k_D s^2) \left(s^2 + \frac{k_1 - \beta_1 - \beta_2}{\alpha_1 + \alpha_2 + 2\alpha_3} \right) = 0. \quad (75)$$

If $k_1 < \beta_1 + \beta_2$ ($\gamma < 1$), the FA robot is unstable at its UEP, since one eigenvalue lies in the open right half-plane.

For the FA robot being linearly controllable at its UEP, when the FA robot is driven into a small neighborhood of the UEP, we need to switch the swing-up controller (42) to a linear state feedback controller to locally stabilize it:

$$\tau = -Fx, \quad (76)$$

where F can be obtained by using pole placement method or Linear Quadratic Regulator (LQR) [9].

In this paper, the small neighborhood of the UEP is defined as

$$w_1 |q_1| + w_2 |q_2| + w_3 |\dot{q}_1| + w_4 |\dot{q}_2| < \varepsilon, \quad (77)$$

where $w_i > 0$, and ε is a small positive constant.

5 Simulation

The mechanical parameters used in this section are the same as those in [7], where $m_1 = 1$ kg, $m_2 = 1$ kg, $l_1 = 1$ m, $l_2 = 2$ m, $l_{c1} = 0.5$ m, $l_{c2} = 1$ m, $J_1 = 0.083$ kg m² and $J_2 = 0.33$ kg m². Using (2) with $g = 9.8$ m/s² yields

$$\alpha_1 = 1.33, \quad \alpha_2 = 1.33, \quad \alpha_3 = 1, \quad \beta_1 = 14.7, \quad \beta_2 = 9.8.$$

We take the torsional stiffness of the spring as $k_1 = 15$. Then, we have $\gamma = 0.612 < 1$ from (9), which does not satisfy the condition in [1] for designing a PD controller to globally stabilize the FA robot at its UEP. From (57), we obtain $\gamma_1 \approx 0.0472$, and we have $\gamma_1 < \gamma < 1$. From Lemma 3, we know that the controller (42) has no singular points if $k_D > 22.8332$. Choose the swing-up controller (42) with $k_D = 36, k_P = 53, k_V = 60$.

In this numerical example, Ω defined in (50) contains two equilibrium points at $q^e = [1.5883, -0.3904]^T$ and $q^e = [-0.5883, 0.3904]^T$. We find that these two equilibrium points both satisfy (67). For validating Lemma 4, we find that the Jacobian matrix evaluated at these two equilibrium points have the same eigenvalues: $-0.9353 \pm 1.1986i, -0.6902, 0.6866$. Since one eigenvalue lies in the open right half-plane, both of them are unstable. Thus, the FA robot approaches W_r according to Statement 1) in Theorem 4. In addition, since $\gamma_1 < \gamma < 1$, the FA robot can approach arbitrarily close to the UEP according to Statement 2) in Theorem 4.

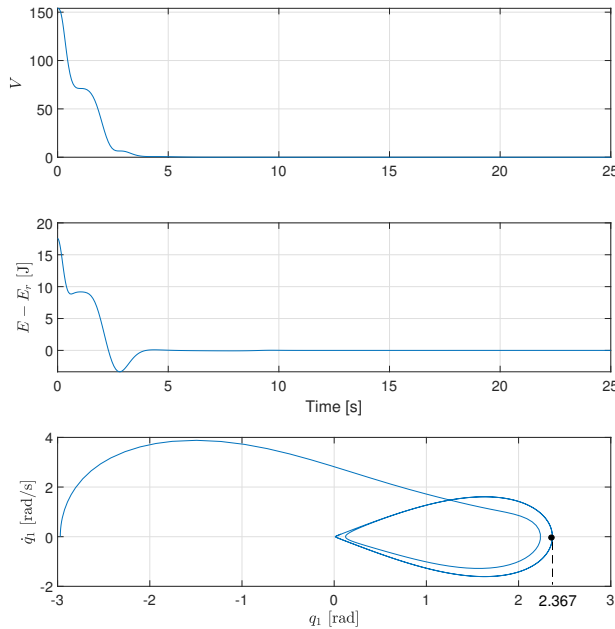


Fig. 6 Time responses of V and $E - E_r$, and the phase portrait of (q_1, \dot{q}_1) under the controller (42).

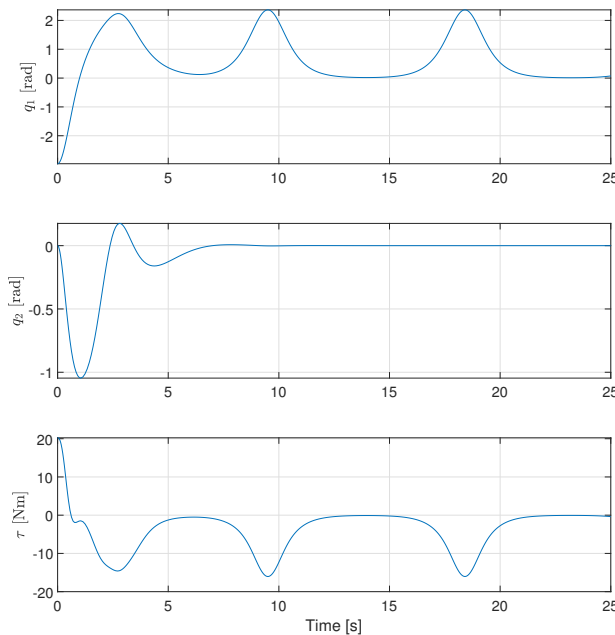


Fig. 7 Time responses of q and τ under the controller (42).

Consider the initial state $x_0 = [-1.4 - \pi/2, 0, 0, 0]^T$. In the swing-up phase, we depict the simulation results in Figs. 6–7. From Fig. 6, we observe that V decreases to 0 and $E - E_r$ approaches 0; also, we know that the FA robot approaches W_r , the phase portrait of (q_1, \dot{q}_1) in which is depicted as Fig. 3(b) with $\phi_1 = 2.367$. From Fig. 7, we know that the first link can be driven to the upright position, and q_2 converges to 0.

Using (11), we have $k_1 \neq k_{uc} = 4.9$. Therefore, the FA robot is linearly controllable at the UEP according to Lemma 2. When the FA robot approaches the small neighborhood of the UEP defined as (77) with $w_1 = w_2 = 1$, $w_3 = w_4 = 0.1$ and $\varepsilon = 0.04$, a stabilizing controller (76) is used to balance it. Take $F = [20.8119, 19.6900, 10.4820, 7.3184]$, which is computed by using the Matlab function “lqr” with $Q = I_4$ and $R = 1$, where I_4 denotes an identity matrix of size 4. As Fig. 8 shows, the switching control strategy can successfully swing up the FA robot and stabilize it at the UEP.

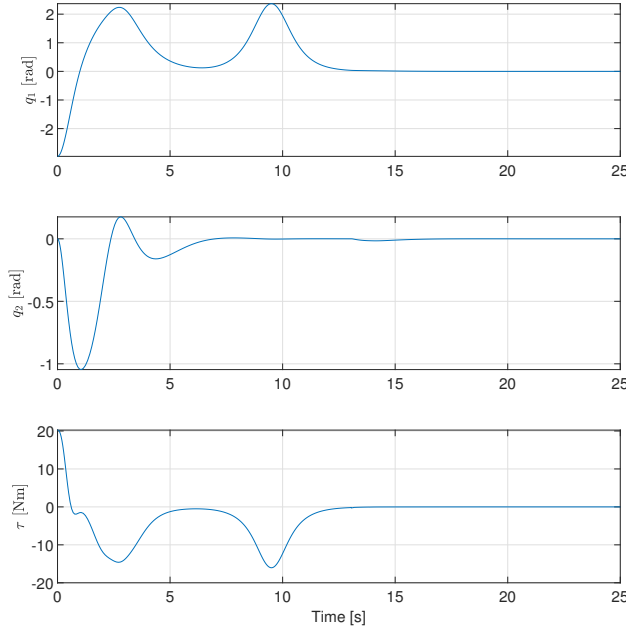


Fig. 8 Time responses of q and τ under the controllers (42) and (76).

6 Conclusion

This paper studied the swing-up control problem for the FA robot moving in a vertical plane. Firstly, for the FA robot around the UEP, we analyzed its linear controllability. Secondly, we proved an important property of the FA robot that if its actuated joint angle is constant under a constant torque, then it is at an equilibrium point. Thirdly, for the FA robot with the torsional stiffness k_1 of the

spring being no greater than the sum of β_1 and β_2 related to the gravitational terms of the robot, since the PD control fails to stabilize it at the UEP, we proposed an energy-based controller having no singular points to swing it up. We analyzed the motion of the FA robot under the energy-based controller by studying the convergence of its total mechanical energy. When the total mechanical energy converges to the desired value, we characterized the phase portrait of the FA robot in terms of the ratio of k_1 and $\beta_1 + \beta_2$. When the convergence is not achieved, we showed that the FA robot approaches an equilibrium point belonging to a set of equilibrium points, and we gave a sufficient condition for checking its instability. From the motion analysis, we presented a sufficient condition such that the FA robot can approach the UEP. Finally, we gave simulation results to show the effectiveness of the proposed controller. In this paper, we not only unified some results about the Acrobot, but also presented some analysis methods, which are expected to be useful in studying other underactuated robots with spring-attached joints.

Appendix A: Proof of Lemma 3

Proof. Notice that (A1) holds if and only if

$$k_D + (E - E_r) M_p(q_2) \neq 0. \quad (\text{A1})$$

We have $(E_r - P(q_1, q_2)) M_p(q_2) \geq (E_r - E) M_p(q_2)$ due to $M_p(q_2) > 0$ and $E \geq P(q_1, q_2)$. Thus, a sufficient condition for (A1) is

$$k_D > \max_{q_1, q_2} \eta(q_1, q_2); \quad \eta(q_1, q_2) = (E_r - P(q_1, q_2)) M_p(q_2). \quad (\text{A2})$$

Next, we show that (A2) is also a necessary condition for (A1). In the case $\max_{q_1, q_2} \eta(q_1, q_2) \geq k_D > 0$, we can always find a state $(q_1, q_2, \dot{q}_1, \dot{q}_2)^T$ for which (A1) does not hold. Letting $(\zeta_1, \zeta_2)^T$ be a value of $(q_1, q_2)^T$ which maximizes $\eta(q_1, q_2)$ and taking $\zeta_d = (\zeta_{1d}, \zeta_{2d})^T$ as

$$\zeta_d = M(\zeta_1, \zeta_2)^{-1/2} \begin{bmatrix} \sqrt{2d_0} \\ 0 \end{bmatrix}, \quad d_0 = \frac{\eta(\zeta_1, \zeta_2) - k_D}{M_p(\zeta_2)} \geq 0 \quad (\text{A3})$$

yields

$$k_D + \left(\frac{1}{2} \zeta_d^T M(\zeta_1, \zeta_2) \zeta_d + P(\zeta_1, \zeta_2) - E_r \right) M_p(\zeta_2) = 0. \quad (\text{A4})$$

Therefore, for the state $(q_1, q_2, \dot{q}_1, \dot{q}_2)^T = (\zeta_1, \zeta_2, \zeta_{1d}, \zeta_{2d})^T$, (A1) does not hold.

Notice that if $E_r - P(q_1, q_2) \leq 0$, then (A2) is guaranteed since $\eta(q_1, q_2) \leq 0 < k_D$. Therefore, for guaranteeing (A2), we just need to evaluate $\max_{q_1, q_2} \eta(q_1, q_2)$ in the case $E_r - P(q_1, q_2) > 0$. This yields

$$\frac{1}{2} k_1 q_1^2 < \beta_1 + \beta_2 - \beta_1 \cos q_1 - \beta_2 \cos (q_1 + q_2) \leq 2(\beta_1 + \beta_2). \quad (\text{A5})$$

Thus, we have

$$|q_1| < 2 \sqrt{\frac{\beta_1 + \beta_2}{k_1}} = \frac{2}{\sqrt{\gamma}}. \quad (\text{A6})$$

Since $\eta(q_1, q_2)$ is periodic in q_2 with period 2π , by using (A6) we know (A2) holds if and only if (43) holds.

Now, suppose that (41) holds. We have $\dot{V} \leq 0$ and V is bounded under the controller (42). According to LaSalle's invariance principle [10] (P.128), we obtain (45). Then, substituting $E \equiv E^*$ and $q_2 \equiv q_2^*$ into (5) proves (46). The detailed proof process is omitted here since the process is similar to the analysis in [14]. This completes the proof of Lemma 3. \square

References

1. Baek, I., Kim, H., Lee, S., Hwang, S., Shin, K.: Swing-up control design for spring attached passive joint Acrobot. *International Journal of Precision Engineering and Manufacturing* **21**(7), 1865–1874 (2020)
2. Fantoni, I., Lozano, R.: Non-linear control for underactuated mechanical systems. Springer (2001)
3. Fantoni, I., Lozano, R., Spong, M.W.: Energy based control of the Pendubot. *IEEE Transactions on Automatic Control* **45**(4), 725–729 (2000)
4. Feliu-Talegon, D., Feliu-Batlle, V.: Passivity-based control of a single-link flexible manipulator using fractional controllers. *Nonlinear Dynamics* **95**(3), 2415–2441 (2019)
5. Hauser, J., Murray, R.M.: Nonlinear controllers for non-integrable systems: The Acrobot example. In: Proceedings of the 1990 American Control Conference, pp. 669–671 (1990)
6. Liu, Y., Xin, X.: Global motion analysis of energy-based control for 3-link planar robot with a single actuator at the first joint. *Nonlinear Dynamics* **88**(3), 1749–1768 (2017)
7. Spong, M.W.: The swing up control problem for the Acrobot. *IEEE Control Systems Magazine* **15**(1), 49–55 (1995)
8. Spong, M.W., Block, D.J.: The Pendubot: a mechatronic system for control research and education. In: Proceedings of the 34th IEEE Conference on Decision and Control, pp. 555–556 (1995)
9. Kailath, T.: Linear systems. Prentice Hall (1980)
10. Khalil, H. K.: Nonlinear systems, Third edn. Prentice-Hall (2002)
11. Troge, H., Steindl, A.: Nonlinear stability and bifurcation theory: An introduction for engineers and applied scientists. Springer (1991)
12. Xin, X.: On simultaneous control of the energy and actuated variables of underactuated mechanical systems—example of the acrobot with counterweight. *Advanced Robotics* **27**(12), 959–969 (2013)
13. Xin, X., Kaneda, M.: Analysis of the energy based swing-up control of the Acrobot. *International Journal of Robust and Nonlinear Control* **17**(16), 1503–1524 (2007)
14. Xin, X., Liu, Y.: A set-point control for a two-link underactuated robot with a flexible elbow joint. *Transactions of the ASME -Journal of Dynamic Systems, Measurement, and Control* **135**(5), 051016-1–051016-10 (2013)
15. Yoshikawa, T., Hosoda, K.: Modeling of flexible manipulators using virtual rigid links and passive joints. *The International Journal of Robotics Research* **15**(3), 290–299 (1996)
16. Zhang, A., Lai, X., Wu, M., She, J.: Nonlinear stabilizing control for a class of underactuated mechanical systems with multi degree of freedoms. *Nonlinear Dynamics* **89**(3), 2241–2253 (2017)
17. Zhang, A., She, J., Li, Z., Pang, G., Liu, Z., Qiu, J.: Nonlinear dynamics analysis and global stabilization of underactuated horizontal spring-coupled two-link manipulator. *Complexity* **2020**, 9096073 (2020)

Statements and Declarations

Funding

This work was supported in part by the National Natural Science Foundation of China under grant number 61973077.

Competing Interests

The authors declare that they have no competing interests.

Author Contributions

All authors contributed to the study conception and design. The first draft of the manuscript was written by [Zhiyu Peng], [Xin Xin] and [Yannian Liu], and all authors commented on previous versions of the manuscript. All authors read and approved the final manuscript.

Data Availability

The authors confirm that the data supporting the findings of this study are available within the article.